Supporting Information

Theoretical Analysis of Tunable Multimode Coupling in a Grating-Assisted Double-Layer Graphene Plasmonic System

Ye Ming Qing, *Hui Feng Ma*,* *and Tie Jun Cui**

State Key Laboratory of Millimeter Waves, School of Information Science and Engineering, Southeast University, Nanjing 210096, China

*Email: hfma@seu.edu.cn; tjcui@seu.edu.cn

Section 1: Dispersion curves of UGSP and LGSP modes

Section 2: Dual-band absorption effect based on UGSP mode and LGSP mode

Section 3: Strong coupling between UGSP mode and LGSP mode

7 pages, 3 figures

1. Dispersion curves of UGSP and LGSP modes

Considering the better absorption performance and avoiding the influence of MP mode, we need to re-optimize the structural parameters. The optimized parameters are P = 240 nm, w = 220 nm, b = 20 nm, h = 400 nm, d_3 = 20 nm, d_2 = 20 nm, and d_1 = 280 nm, respectively.

For the four-layer system, the dispersion relation of UGSP mode can be obtained by solving Eq. (3). Similarly, for the five-layer system, the dispersion relation of LGSP mode propagates in the waveguide can be calculated by Eq. (7). Note that the wavevector (i.e., β_U or β_L) of graphene plasmonic wave is much larger than that of incident light in free-space, UGSP mode or LGSP mode cannot be excited directly. Herein, the silver grating is used to compensate the wavevector mismatches. For a normal incidence wave, the resonant condition is determined by Eq. (4). As shown in Figs. S1(a) and S1(b), the phase of the silver grating intersects with the theoretical dispersion curves of the UGSP mode and LGSP mode, which predicts the resonant wavelengths. However, the dispersion curves of UGSP mode and LGSP mode are different, so two resonant wavelengths are generated under the same Fermi energy. For example, when $E_{F1} = E_{F2}$ = 0.75 eV, the theoretical fundamental resonant wavelengths of UGSP mode and LGSP mode are about 9 μm and 10 μm, respectively, which provides a prerequisite for dual-band absorption.

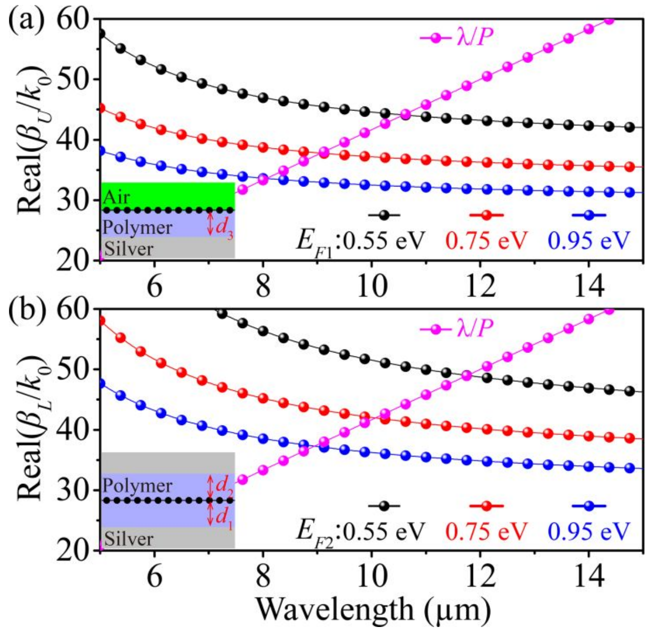

Figure S1. (a) Dispersion curves of UGSP modes for the four-layer system. (b) Dispersion curves of LGSP modes for the five-layer system.

2. Dual-band absorption effect based on UGSP mode and LGSP mode

Figure S2(a) illustrates the absorption spectra of the hybrid system with/without double-layer graphene when E_{F1} = E_{F2} = 0.75 eV. Obviously, no resonant mode is supported in the considered wavelength range when the hybrid system is free of graphene. However, by introducing upper- and lower-layer graphene into the system, dual-band absorption effect occurs. The quasi-linear superposition of the two modes forms two nearly perfect absorption peaks at 8.9 μm and 9.97 μm, and the corresponding resonance positions are basically consistent with the theoretical results. The electric field distributions ($|E|$ and E_x) at two resonant wavelengths are respectively shown in Fig. S2(b). The phase matching between the propagating plasmonic wave and incident wave is satisfied by the assistance of silver grating. The UGSP mode traps its electromagnetic energy near upper-layer graphene without any overlap to lower-layer graphene, so does

LGSP mode. The double propagating plasmonic waves not only realize dual-band perfect absorption, but also achieve selective enhancement of the electric fields.

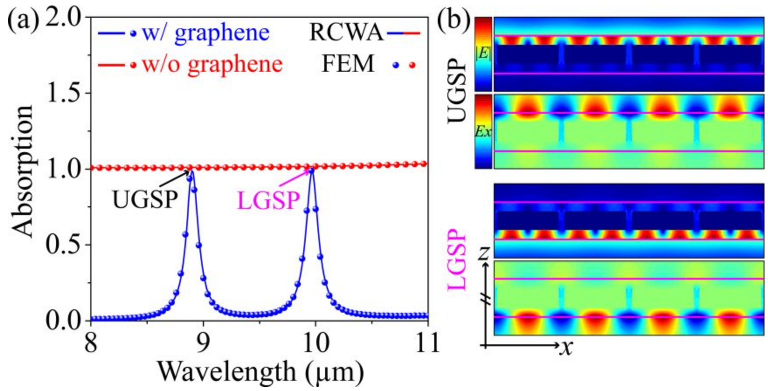

Figure S2. (a) Absorption spectra for the hybrid system with/without double-layer graphene when E_{F1} = E_{F2} = 0.75 eV. (b) Electric field distributions (|E| and E_x) of the hybrid system at the two resonant wavelengths, corresponding to the UGSP mode and LGSP mode, respectively. The magenta lines denote two graphene sheets.

3. Strong coupling between UGSP mode and LGSP mode

Figure S3(a) shows the absorption spectra of the hybrid system with various Fermi energy of the double-layer graphene (i.e., E_F = E_{F1} = E_{F2}). When E_F increases, the resonant wavelengths undergo significant blueshift. Moreover, the excellent spectral distributions with high absorption and low sideband are well maintained. The theoretical predicted resonant wavelengths are shown by the green marks, which are in good agreement with the simulation results. In the results shown in Fig. S3(b), as E_F increases from 0.65 to 0.85 eV with an increment of 0.1 eV, the spectral separation for resonant wavelengths of the UGSP mode (left) and the LGSP mode (right) decreases. No coupling or hybridization between the two resonant modes. Therefore, a dual-band absorber with excellent spectral characteristics (i.e., controllable wavelength separation, low sideband, and high absorption) can be achieved by adjusting E_F of the double-layer graphene simultaneously.

The coupling and hybridization between the plasmonic modes give rise to many interesting phenomena, exhibiting excellent energy transfer characteristics and prominent light manipulation. A simple method to achieve the interaction between UGSP and LGSP modes is to adjust Fermi energy of each graphene separately. Figures S3(c) and S3(e) clearly show that the interaction characteristics of the plasmonic modes are efficiently tuned by separately altering the Fermi energy of the upper- and lower-layer graphene. Taking Fig. S3(c) as an example, the Fermi energy in lower-layer graphene is fixed at E_{F2} = 0.8 eV, while the Fermi energy of upper-layer graphene increases from 0.4 to 1.0 eV. As E_{F1} increases, the UGSP mode successfully couples with the LGSP mode, resulting in two hybrid polariton modes. The two dispersive polariton bands do not cross each other, but undergo an anticrossing with an energy gap of 4.1 meV (i.e., Ω = 1 THz). The coupling behavior can also be achieved by adjusting E_{F2} independently, while E_{F1} keeps constant, as shown in Fig. S3(e).

According to the coupled oscillator model, the dispersion relations of the two hybrid modes (green round marks) are calculated and plotted in Figs. S3(c) and S3(e). In addition, we get the mixing fractions of UGSP and LGSP mode in the hybrid bands. For example, in Fig. S3(d) for HPB, with the increase of E_{F1}, the mixing fraction of the UGSP mode ($|\alpha_U|^2$) increases and that of the LGSP mode ($|\alpha_L|^2$) decreases. When E_{F1} < 0.64 eV, the HPB mainly comes from LGSP mode, corresponding to the larger $|\alpha_L|^2$. However, the mixing fraction of UGSP mode eventually exceeds that of the LGSP mode when E_{F1} > 0.64 eV, indicating that the HPB mainly comes from UGSP mode. Particularly, the intermediate state at E_{F1} = 0.64 eV corresponds to the hybrid modes with identical fractions of UGSP mode and LGSP mode (i.e., $|\alpha_U|^2 = |\alpha_L|^2$). For LPB in Fig. S3(d), the trend of mixing fractions is contrary to that of HPB.

Figure S3(g) shows the electric field $|E|$ patterns of resonant wavelengths in the HPB at E_{F1} = 0.5, 0.64, and 0.8 eV (corresponds to the star marks in Fig. S3(c)). When E_{F1} = 0.5 eV, the electromagnetic field is trapped mainly at the lower-layer graphene, similar to a LGSP mode, and the electric fields at the upper-layer graphene are weak. Hence, we call this hybrid mode a LGSP-like mode. In the case of E_{F1} = 0.64 eV, the energy of electric field is harvested by the upper- and lower-layer graphene with identical mixing fractions, indicating that the UGSP mode and the LGSP mode can be excited simultaneously. Hence, this hybrid mode can be represented by Half-LGSP mode (or Half-UGSP mode). When E_{F1} = 0.8 eV, the electric field localized at upper-layer graphene is quite similar to a UGSP mode, so we call this hybrid mode an UGSP-like mode. Obviously, the system can construct an effective optical switch based on the characteristics of UGSP-LGSP coupling.

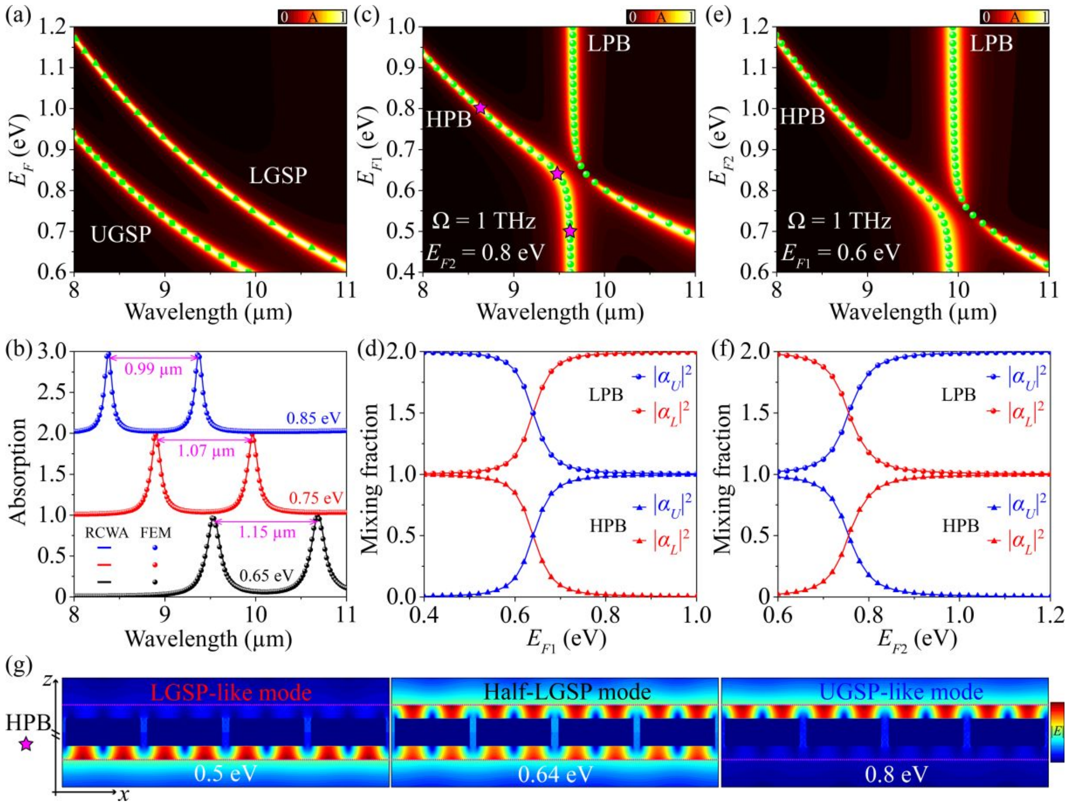

Figure S3. (a) Absorption contours of the plasmonic system as a function of incident wavelength and Fermi energy (E_F = E_{F1} = E_{F2}). The green marks are the theoretical predictions. (b) Simulated absorption spectra with E_F varying from 0.65 to 0.85 eV with an increment of 0.1 eV. (c, e) Absorption spectra as a function of the wavelength and Fermi energy. The initial values of E_{F2} and E_{F1} are 0.8 eV and 0.6 eV, respectively. The round markers represent the resonant positions of the hybrid modes calculated by the two-oscillator model. (d, f) The mixing fractions of the UGSP mode and LGSP mode in the polariton bands as a function of Fermi energy. (g) The corresponding electric field $|E|$ patterns of resonant wavelengths in the HPB at E_{F1} = 0.5, 0.64, and 0.8 eV, respectively.